Desalination 533 (2022) 115764

Contents lists available at ScienceDirect

Desalination

journal homepage: www.elsevier.com/locate/desal

Regenerative electrochemical ion pumping cell based on semi-solid electrodes for sustainable Li recovery

Daniel Perez-Antolin [a,b], Cristina Irastorza [c], Sara Gonzalez [a], Rebeca Moreno [c], Enrique García-Quismondo [c], Jesús Palma [c], Julio J. Lado [c,**], Edgar Ventosa [a,b,*]

[a] Department of Chemistry, Universidad de Burgos, Pza. Misael Bañuelos s/n, E-09001 Burgos, Spain
[b] International Research Centre in Critical Raw Materials-ICCRAM, University of Burgos, Plaza Misael Bañuelos s/n, E-09001 Burgos, Spain
[c] Electrochemical Processes Unit, IMDEA Energy, Avda. Ramón de la Sagra 3, 28935 Móstoles, Madrid, Spain

HIGHLIGHTS

- A new electrochemical ion separation concept is developed.
- The use of semi-solid electrode largely facilitates the regeneration of the system.
- The use of semi-solid electrodes provides versatility to change the target ion.
- Cheap microporous separators are also used to confine the electroactive materials.
- Tunable porosity of semi-solid electrodes enables high areal capacities.

ARTICLE INFO

Keywords:
Ion separation
Electrochemical methods
Intercalation materials
Semi-solid electrodes
Ion pumping

ABSTRACT

Demand of lithium is expected to increase drastically in coming years driven by the market penetration of electric vehicles powered by Li-ion batteries, which will require faster and more efficient Li extraction technologies than conventional ones (evaporation in brines). The Electrochemical Ion Pumping Cell (EIPC) technology based on the use of Faradaic materials is one of the most promising approaches. However, its relatively short lifespan prevents its commercial deployment. Herein, a new EIPC concept based on the use of semi-solid electrodes is proposed for the first time, which takes advantage of the rheological characteristics of semi-solid electrodes that enable simple and cheap regeneration of the Regenerative Electrochemical Ion Pumping Cell (REIPC) systems after reaching its end-of-life. A proof-of-concept for REIPC is accomplished by simple replacement of the semi-solid electrode demonstrating a remarkable electrochemical performance (e.g. 99.87%cycle^{-1}, 99.98%h^{-1}, 3–4 mAh cm^{-2}) along with a competitive ion separation (e.g. 16.2 mgLi·g$_{NiHCF}^{-1}$, 4 g$_{Li}$ m^{-2} and 15.6 Wh·mol^{-1}). The use of semi-solid electrode offers other unique features such as a significant cost reduction of 95% for every regeneration regarding conventional EIPC, proving that REIPC concept successfully addresses the issues associated to the sustainability and recyclability of the conventional EIPC's for lithium capturing.

1. Introduction

The lithium demand has been increasing in the last years, mainly due to the growth of portable electronics powered by Li-ion batteries. If projections are fulfilled, the penetration of electric vehicles will boost lithium demand in near future. In this sense, different financial studies estimated a total lithium demand of 278 kt of Lithium Carbonate Equivalents (LCE) in 2018, for which demand associated to lithium-ion batteries (LIB's) represents 58% of that amount [1]. These studies also project the total lithium demand to reach 2.20 Mt. LCE in 2030. The 10-fold increase in lithium demand with respect to 2018 is mainly triggered by battery applications related with the electric mobility. This estimation is supported by a recent report published by the International Energy Agency that indicates an increase of the vehicle battery capacity from 170 GWh per year (2020) to 1.5 TWh in 2030 following the Stated Policies Scenario, and even reaching the 3 TWh in a Sustainable

* Corresponding author at: Department of Chemistry, Universidad de Burgos, Pza. Misael Bañuelos s/n, E-09001 Burgos, Spain.
** Corresponding author at: IMDEA Energy, Av. Ramón de La Sagra, 3, 28935 Móstoles, Madrid, Spain.
E-mail addresses: julio.lado@imdea.org (J.J. Lado), eventosa@ubu.es (E. Ventosa).

https://doi.org/10.1016/j.desal.2022.115764
Received 11 January 2022; Received in revised form 1 April 2022; Accepted 1 April 2022
Available online 12 April 2022

Development Scenario. [2] Currently, there are two main lithium sources; *i)* brines of high-altitude salt flats known as "salars" (which are mainly found in Bolivia, Argentina and Chile), and *ii)* hard rock spodumene deposits. Salars are usually located in areas of geothermal activity and present relatively high concentration of dissolved lithium (30–150 mg L^{-1}, [3]). In salars, the lime-soda evaporation is the most employed extraction process. This practice basically consists on pumping the brines from under the saline crust to solar evaporation ponds from which concentrated brine is treated with precipitation agents, e.g. sodium carbonate, for obtaining first lithium carbonate and then lithium hydroxide [3]. Here the main drawbacks associated to lithium extraction from brines are the long processing times, the low lithium recovery efficiency, the weather dependency and the high consumption of water [4]. These limitations affect the lithium global production capacity from brine, estimated 120.5 Ktons/year [4] which, according to predictions, will not be enough to cover the lithium market demand in the near future [5,6]. In this context, the quest for more convenient technology has become of great interest. Thus, emerging technologies are expected to involve environmentally friendly methodologies looking for reducing wastes production, maximizing the areal capacity of evaporating ponds and minimizing the chemicals consumption [7].

Different approaches have been explored to tackle this challenge searching for a relatively high selective separation that consumes a moderate amount of energy at a reasonable cost. In this regard, the electrochemical technologies have recently attracted the attention of the scientific community [3,5,6,8–13]. Ions from a stream are captured by selective electrodes through electrochemical reactions which enables the production of a diluted stream and a concentrated stream. First electrochemical technologies employed capacitive electrodes in which ion separation is driven by the formation of the electrical double layer (EDL) [9, 14–19]. However, this physical and non-selective process leads to limited ion storage capacity and a low separation factor [9]. More recently, the use of Faradaic intercalation materials was proposed for electrochemical ion pumping. These materials, typically used in batteries for energy storage, [8,20,21] are able to intercalate selectively certain ions within their structures as a result of a redox reaction [21,22]. Consequently, intercalation electrodes present high ion selectivity and specific charge capacity with respect to capacitive electrodes [20,23] which results from the bulk redox reactions in contrast with surface confined reactions for capacitive materials. However, same as in batteries, insertion of ions into the bulk of intercalation materials leads to accelerated degradation in comparison to capacitive processes [9], which may compromise the techno-economic feasibility and sustainability of Faradaic-based ion separation systems.

Faradaic intercalation materials are usually fixed on the electrode surface located inside the electrochemical reactor forming a porous and immobile film. Recently, intercalation materials have been deployed in the field of redox flow batteries in the form of flowable "semi-solid electrodes" (mixture of solid intercalation material, carbon additive and electrolyte in the absence of binder) [24,25]. By doing this, solid Faradaic intercalation materials can be stored in external reservoirs and pumped into the reactor for energy conversion enabling decoupling of energy and power. Despite semi-solid electrodes were conceived for redox flow batteries, their unique feature can be of great interest for other applications.

Herein an innovative electrochemical ion pumping cell concept having easily exchangeable Faradaic semi-solid electrodes is proposed for facilitating regeneration and direct reuse of the system. The use of semi-solid electrodes containing intercalation materials allows simple substitution of the spent Faradaic electrodes when it reaches its end of life. Two cell designs are developed for implementing the proposed concept of Regenerative Electrochemical Ion Pumping Cell (REIPC): *i)* a configuration using two Li-selective intercalation materials and an ion-selective membrane and *ii)* a membrane-free configuration using one Li-selective and one Na-selective intercalation materials. Both prototypes were fabricated showing to deliver good ion separation properties and, more importantly, to be easily regenerated by replacing Faradaic materials in the form of semi-solid electrodes and, thus, enabling the reuse of the entire system.

2. Materials and methods

2.1. Reagents and materials

Lithium Iron Phosphate ($LiFePO_4$, Advanced Lithium Electrochemistry), Carbon black (KetjenBlack EC-600 JD, Azelis and AkzoNovel polymer chemicals), Lithium Manganese Oxide ($LiMn_2O_4$, Nanomyte NEI Corporation), Lithium Chloride (LiCl, Alfa Aesar), Sodium Chloride (NaCl, Sigma Aldrich), Potassium Chloride (KCl, Sigma Aldrich), Magnesium Chloride ($MgCl_2$, Alfa Aesar) were used as received. Potassium Nickel Hexacyanoferrate ($KNi[Fe(CN)_6]$) was synthetized following the route described by [11], briefly, 120 mL of $Ni(NO_3)_2{\cdot}6H_2O$ (Alfa Aesar) 0.1 M and 120 mL of $K_3Fe(CN)_6$ 0.05 M (Alfa Aesar) were added simultaneously to 60 mL of water while stirring at 70 °C forming a brown precipitate. The suspension was sonicated for 30 min at 70 °C, and rested overnight. The precipitate was filtrated and washed with distilled water, and subsequently dried in vacuum at 70 °C. X-ray diffraction pattern of the obtained materials confirming that the synthesis was carried out successfully is provided in Section S1, Fig. S1. XRD analysis was carried out at IMDEA Energy using a Philips PW 3040/00 X'Pert MPD/MRD diffractometer with Cu Kα radiation ($\lambda = 1.54178$ Å).

Expanded graphite (Sigracell TF6) was used as current collector, Celgard 3501 as separator, and Fumasep FAA-3-30 as selective anionic exchange membrane (AEM). The external case of the battery was fabricated by 3D-Printing machine (MakerBot ReplicatorTM 2×) using ABS as plastic material.

2.2. Preparation of semi-solid electrodes

Semi-solid electrodes containing a mixture of the active material (77 wt%, 195 mg/mL electrolyte), carbon black additive (23 wt%, 58.3 mg/mL electrolyte) and electrolyte (6 mL) were prepared directly in a syringe by stirring with a high-shear homogenizer (Ultra-Turrax IKA T18-Basic) during three periods of 10 min resting 5 min between periods. The electrolyte used for each experiment had the same composition as the initial brine solution.

2.3. Electrochemical cell

A filter-pressed type electrochemical cell was designed using the following elements: 3-D printed end plates, expanded graphite current collectors, Viton gaskets with the intentionally cavities for allocating the semi-solid electrodes and Celgard separator for confining solid particles. Moreover, another gasket was used for allowing the electrolyte flow through the mentioned cell. This description corresponds to half-cell configuration since the same layers were used for the other half-cell that allowed to assemble the complete device. Where anion AEM was used, it was located in the middle of the water-flow-channel. Details of the design and construction of the electrochemical cell used are provided in Section S2, Supp. Info.

A Masterflex® L/S® peristaltic pump with two heads was used for pumping the electrolyte flow through the device at 100 mL·min^{-1}.

2.4. Electrochemical measurements

Galvanostatic measurements as well as electrochemical impedance spectroscopy measurements were carried out using an EC-Biologic potentiostat. The proof of concept for the REIPC containing $LiFePO_4$ - $FePO_4$ was performed by cycling the system between 0.35 V and − 0.35 V at 2 mA cm^{-2}. Regarding the demonstration of the REIPC electrode substitution, the cell was cycled between 0.5 V and − 0.5 V at 2 mA cm^{-2} after each one of the electrode substitutions (even for those with

capacitive behavior). In the case of the proof of concept for the asymmetrical configuration, the $LiFePO_4$ - $LiMn_2O_4$ REIPC was cycled between 0 V and 0.8 V at 2 mA cm^{-2}. Moreover, the $LiMn_2O_4$ – KNi[Fe $(CN)_6$] Membrane-Free REIPC (MF- REIPC) was cycled between 0 V and 1 V at 1 mA cm^{-2}.

Ion chromatography (IC) analysis (930 Compact IC Flex, Metrohm) was performed to evaluate the variation of the lithium concentration in the electrolytes and determined the lithium adsorption capacity (SAC_{Li}). Additionally, Flame photometer (Corning 410) was used for measuring the concentration of lithium and sodium in the electrolytes of Membrane-Free Regenerative Electrochemical Ion Pumping system.

2.5. Figures of merit

Four figures of merit are defined to assess the performance of the prototypes:

The efficiency of the system (η) is defined as the ratio between the change in concentration of cations effectively achieved for the stream and the theoretical change in concentration of cations corresponding to the charge consumed by the system, following the Eqs. (1) and (2), for lithium capturing and releasing process respectively [26].

$$\eta = \frac{C_i \cdot V - |Q|/F}{C_f \cdot V} \tag{1}$$

$$\eta = \frac{C_f \cdot V}{C_i \cdot V + |Q|/F} \tag{2}$$

In which *Ci* and Cf (mol L^{-1}) are the initial and the final concentrations, respectively, *V* is the volume of the electrolyte solution (L), *Q* (C) is the charge consumed by the system and *F* is the Faraday constant.

The lithium adsorption capacity (SAC) is defined as the amount of Li removed per mass of Faradaic intercalation material, and was calculated using the Eq. (3)

$$SAC_{Li} = \frac{m_{Li}}{m_e} \tag{3}$$

where m_{Li} (mg) is the amount of lithium removed and m_e (g) the mass of the limiting electrode.

The adsorption areal capacity (AAC) is defined as the amount of Li removed per electrode area, and was calculated using the Eq. (4)

$$AAC = \frac{m_{Li}}{A} \tag{4}$$

where A (cm^2) is the area occupied by the electrode limited by the gasket.

The energy consumption is defined as the net energy consumed by the systems to remove a mole of Li^+. The calculation differs depending on configuration of the systems. I) In symmetrical systems, e.g. $LiFePO_4$ – $FePO_4$, the device is separating ions in a continuous mode so that there is no need for half-cycles. Thus, the energy consumption is defined as the energy needed for one half-cycle normalized by the amount of Li^+ recovered in such a half-cycle. On the one hand, energy is stored in an asymmetrical system, i.e. energy is consumed and released during the charge process and discharge process respectively. Therefore, the second half-cycle does not consume energy, but it releases it. Therefore, the net energy consumption is calculated as the difference between the energy applied and released normalized by the amount of Li^+ recovered during the entire cycle.

The selectivity coefficient of lithium ions versus *sodium ions ($K_{Li,Na}$)* is defined as the change in Li concentration normalized by the total change in concentration of cations (Eq. (5)). This coefficient varies between 0 and 1.

$$K_{Li,Na} = \frac{\Delta C_{Li}}{\Delta C_{Li} + \Delta C_{Na}} \tag{5}$$

Li recovery rate (R_{Li}) is defined as the mass of Li recovered (ΔC_{Li}) per area of electrode (A) and unit of time (t), as describe in Eq. (6)

$$R_{Li} = \frac{\Delta C_{Li}}{A^* t} \tag{6}$$

3. Results and discussion

3.1. The concept of Regenerative Electrochemical Ion Pumping Cell (REIPC)

The Electrochemical Ion Pumping Cell (EIPC) is a device that makes use of ion uptake and release driven by redox reactions occurring in Faradaic materials (typically used in batteries) for driving ion separation in a stream. By doing this, the concentration of targeted ions in a solution is modified. The EIPC concept has been proposed to improve the separation of Li-ions in the lithium capturing process using brines [10,27]. Since there are several metal cations in this type of streams, e.g. Li^+, Na^+, K^+, the EIPC needs selectivity towards Li-ions. This selectivity is achieved by using one of two following options: i) two Li-selective Faradaic electrodes and an AEM or ii) two Faradaic electrodes each one having selective towards different cations without membrane. Each option requires a specific setup and operating mode offering intrinsic advantages and disadvantages. Fig. 1a illustrates the necessary steps in an EIPC containing ion-selective membrane to concentrate Li-ions. The intercalation materials used in the two electrodes are selective towards Li-ions being separated by an AEM. During the first step (first half-cycle), Li-ions are captured in compartment A by electrode A as Li-ions are released in compartment B from electrode B. To maintain electroneutrality, anions move from compartment A to compartment B. As a result, the concentration of Li-ions in the streams exiting compartment A and compartment B is diluted and concentrated, respectively. In the second step (second half-cycle), the opposite processes occur; concentration of Li-ions increases in compartment A while it decreases in compartment B. Fig. 1b shows the steps for an EIPC containing two intercalation materials, each of which is selective towards a different cation. In this case, two streams (one concentrated and one diluted) are not continuously obtained as in the previous operating mode. In the first step (first half-cycle), Li-ions are released from electrode B while another cation (e.g. Na-ions) is captured by electrode A resulting in one single stream with higher concentration of Li-ion and lower concentration of Na-ions. In the second step (second half-cycle), Li-ions are captured by electrode B while Na-ions are released from electrode A resulting in a stream with lower concentration of Li-ion and higher concentration of Na-ions.

In both configurations of the EIPC above-explained, ion-capturing Faradaic materials are fixed onto the current collectors, which are sealed inside the cell. Degradation of these materials and/or occurrence of parasitic reactions leading to charge unbalancing between positive and negative electrode materials, e.g. oxygen reduction reaction, are responsible for reaching end-of-life and for the need for recycling of the entire system. In contrast to conventional cell configurations, the REIPC concept proposes that an electrochemical cell is pre-assembled. Cavities are intentionally created next to the current collectors, which are then filled with semi-solid electrodes (Fig. 2). Once semi-solid electrodes are injected, the electrochemical cell is sealed and operated normally until it reaches its end-of-life. The flowable nature of semi-solid electrodes (Section S3, Fig. S4, Supp. Info.) allows for direct and easy replacing of spent electrodes at the end-of-their-life by fresh electrodes through a dejecting-reinjecting process (Fig. 2). In this fashion, spent electrodes are directly recovered, and the entire cell is reused. It should be noted

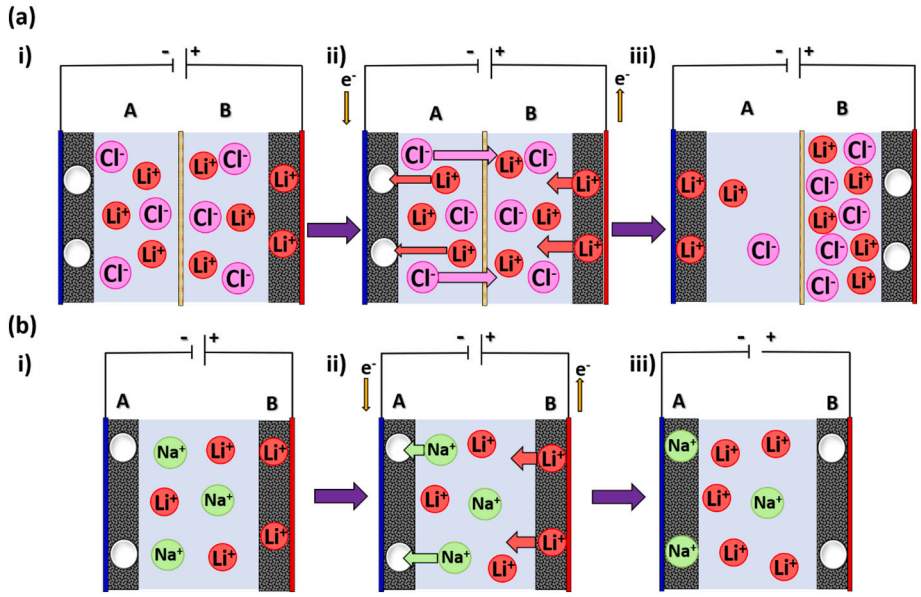

Fig. 1. Illustration of two operating modes for the EIPC for the first half-cycle resulting in the concentration of Li-ions. (a). EIPC with ion-selective exchange membrane (b) Membrane free EIPC.

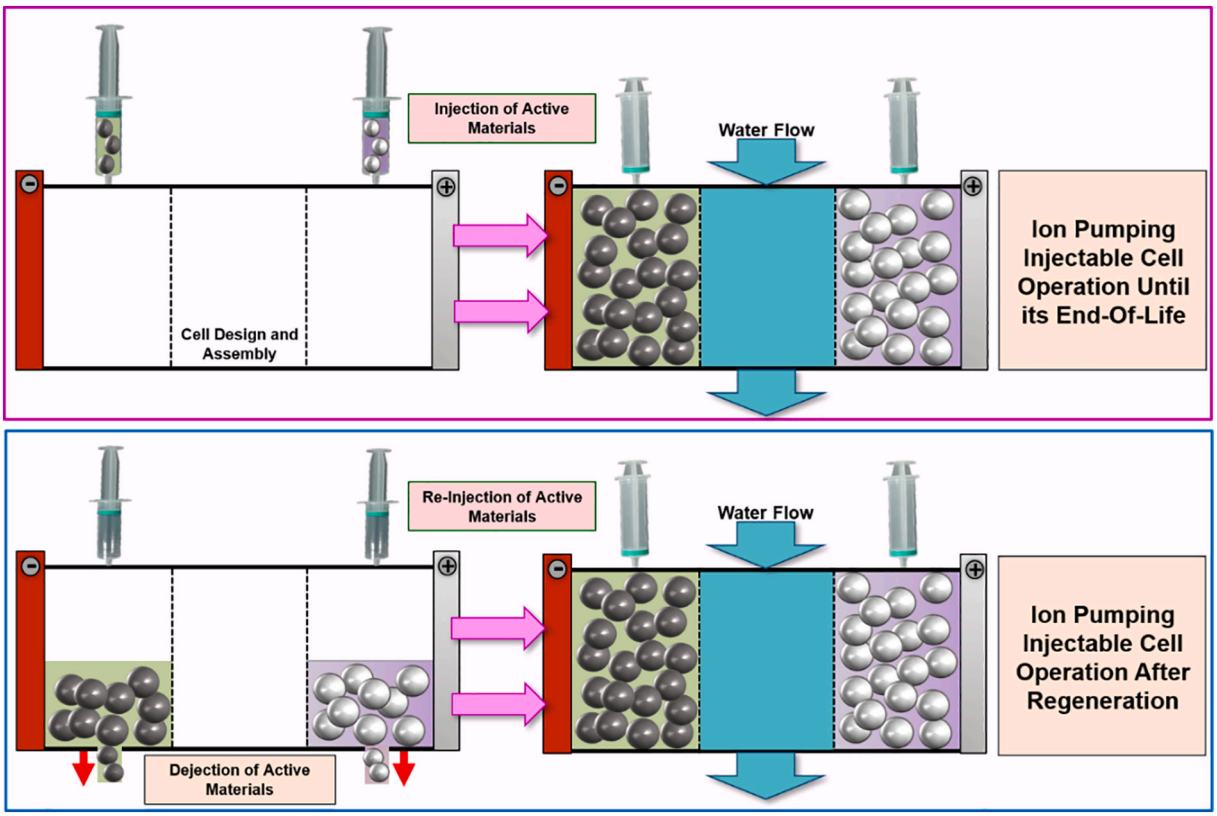

Fig. 2. Process of substitution (injection and dejection) of the semi-solid electrodes into a pre-assembled cell for their use in ion pumping applications.

that flowable semi-solid electrodes remain static during operation of the REIPC. Only the stream of Li brine flows through a compartment that is located between the two electrodes. Confinement of semi-solid electrodes is proposed through the use of microporous separators and gaskets, avoiding by size exclusion, that particles of the electrode are dragged into the flowing solution. It should be also noted that previous reports related to the use of semi-solid electrodes for ion separation requires continuous flow of slurry [28]. That configuration does not offer as many techno-economically advantages as REIPC, mainly due to degradation of the devices (erosion by the flowing suspended particles) and high energy consumption (pumping of viscous and dense fluids).

Pictures of the actual device shows (Fig. 3a) the different elements of the cell, (Fig. 3b)the injection of semi-solid electrodes in the cell, and (Fig. 3d) the final assembled systems including peristaltic pumps. Simplified schemes of the system are shown in Figs. S2 and S3.

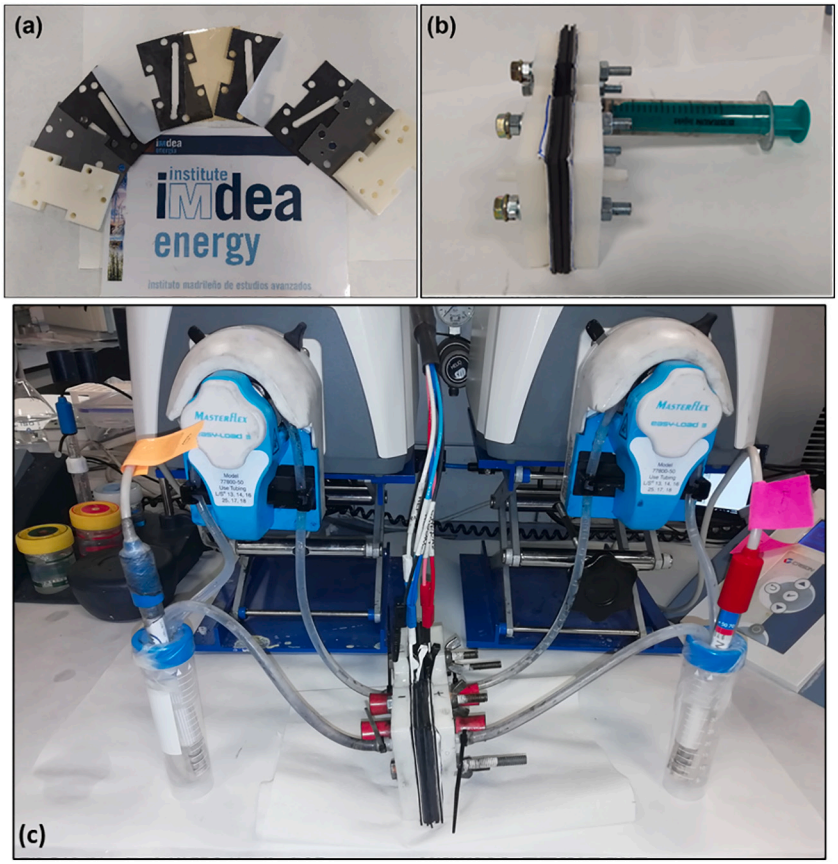

Fig. 3. Pictures of (a) the different components of the Regenerative Electrochemical Ion Pumping Cell (3D Printed ABS Endplate, Graphite Current Collector, Viton Gasket, Microporous Separator C350, Anion Exchange Membrane (AEM), (b) regeneration process by dejection / injection of semi-solid electrode from / into the assembled REIP cell, (c) operating REIP system.

3.2. Membrane-Containing Regenerative Electrochemical Ion Pumping Cell (MC-REIPC)

A MC-REIPC was assembled using an anion-selective membrane and two Li-selective Faradaic materials ($LiFePO_4$ (LFP) and $FePO_4$ (FP)) in the form of flowable semi-solid electrodes. First, one LFP semi-solid electrode was injected and oxidized inside the cell to obtain the de-intercalated material (FP) (Fig. S2 path A, Supp. Info.). Details of this oxidation process ("activation") are provided in the Supp. Info. (Section S3). Then, the second flowable semi-solid electrode (LFP) was injected in the opposite side of the cell (Fig. S2 path B, Supp. Info.). This "activation" step might be skipped if active materials are injected in its oxidized and reduced forms. Once electrodes were injected and "activated", the electrolyte solution was pumped from two solution tanks using a peristaltic pump passing through the cell by independent paths (Fig. S2 Supp. Info. path CF and path DE). The proof-of-concept was performed using a batch configuration (also known as recirculation mode) in which the electrolyte was returning to the feed solution containers after completing the flow circuit.

Our hypothesis here is that the use of the MC-REIPC equipped with semi-solid electrodes enables an easy regeneration of the system through substitution of spent Faradaic materials. Thus, several subsequent regenerations that consisted of dejection and reinjection of semi-solid electrodes were performed in an REIPC cell using LFP-FP semi-solid electrodes to demonstrate this major advantage. Fig. 4a shows the results of an experiment designed to visualize the effective replacement of semi-solid electrode: R1) LFP semi-solid electrode was replaced by a fresh one. An increase of ca. 30% in charge storage capacity was observed which means that the battery almost fully recovered the initial capacity after the replacement of electrode. R2) LFP semi-solid electrode was replaced by activated carbon semi-solid electrode leading to an enormous capacity drop, which also shows the limited contribution of the activated carbon to the charge storage in comparison with LFP. R3) Both semi-solid electrodes were again replaced by fresh LFP and FP semi-solid electrodes. Charge storage capacity increased to the initial values (3–4 mAh cm^2). R4) LFP semi-solid electrode was again replaced by activated carbon semi-solid electrode leading again to a substantial decrease of the capacity. R5) In the last regeneration, fresh LFP semi-solid electrode was injected recovering value of capacity in the order of 3–4 mAh cm^{-2}.

Fig. 4b displays the voltage profiles of the cell initially assembled and after the replacement of one LFP semi-solid electrode by activated carbon semi-solid electrode. Prolonged measurements of REIPC (without regeneration processes) showed excellent cycle stability at 3 mAh cm^{-2} delivering capacity fading of 0.0048% per cycle and 0.0016% per hour, with an exceptional coulombic efficiency >99% over at least 50 cycles and 150 h (Section S5, Fig. S5). Importantly, results displayed in Fig. 4 confirmed that the easy recycling process of the active materials for our REIPC system enables direct reuse of the cell after reaching end-of-life of the electrodes. Since all the expensive components of the cell such as ion-selective membranes and current collectors are reused, the concept of REIPC contributes significantly to cost reductions. According to our estimations (Section S6, Supp. Info.) a cost reduction of 95% is achieved in each regeneration by implementing the REIPC concept.

It should be noted that the symmetrical configuration using LFP-FP semi-solid electrodes do not effectively store energy while capturing ions since both electrodes have the same standard redox potentials leading to a nominal cell voltage of 0 V. To store energy, two ion-intercalation materials having different redox potentials should be employed. Indeed, energy storage in ion separation systems represent an

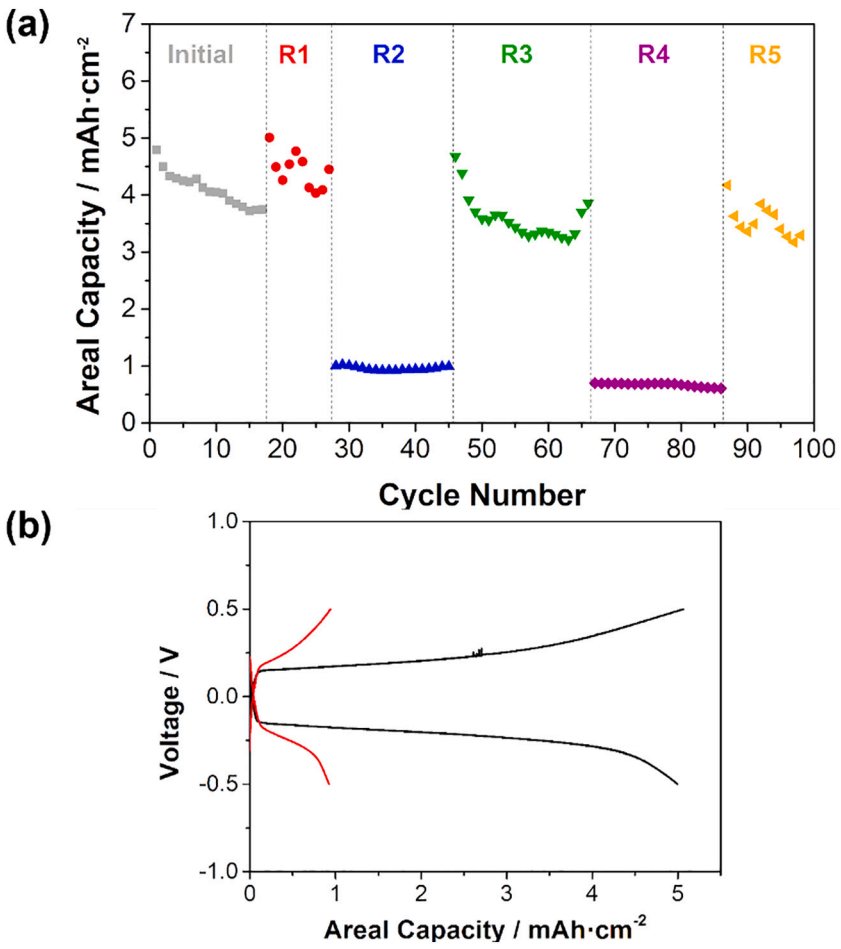

Fig. 4. Performance of the REIPC LFP-FP cell. (a) after several injections and reinjections with activated carbon and LFP. (b) Comparison between capacitive (Activated Carbon-Activated Carbon, red line) and Faradaic (LFP-FP, black line) REIPC Cells. Note that areal capacity (mAh cm^{-2}) is estimated as the accumulated charge (mAh) provided by the potentiostat during one step normalized by the geometric area of the electrodes. (For interpretation of the references to colour in this figure legend, the reader is referred to the web version of this article.)

additional benefit of this technology. In our case (Section S7, Supp. Info.), the REIPC containing LMO and FP semi-solid electrodes delivered an average discharge cell voltage of 0.28 V (Fig. S10a), a capacity fading of $4{\cdot}10^{-5}$% per cycle and $3{\cdot}10^{-5}$% per hour (Fig. S10b) and reversible specific energy of 8.9 Wh kg_{LMO}. Thus, this successful measurement demonstrates the versatility of the REIPC technology on using different electrode materials and configurations (symmetric vs asymmetric cell).

After the evaluation of charge storage capacity and regeneration capacities, the ion separation capability of the proposed concept was investigated. The selectivity of LFP towards Li-ions has been exploited for selective lithium extraction in the presence of other metal cations [3,8,12,29]. The ion separation process consists of two steps as discussed generally in Fig. 1a, and specifically for the case of LFP-FP in the Supp. Info. (Section S9, Fig. S12). In the first step (half-cycle) LFP semi-solid electrode is oxidized releasing Li-ions and FP is simultaneously reduced capturing Li-ions while Cl-ions moves from FP compartment to LFP side through the AEM. In this way, two streams containing different Li-ion concentrations are obtained: Li-ion concentrated stream in the LFP compartment and Li-ion diluted stream in the FP side. In this configuration, the REIPC can be operated continuously resulting in two streams. Qualitatively, variations in the concentration of LiCl were monitored using the ionic conductivity of the two streams. Fig. 5a shows the evolution of the cell voltage together with the ionic conductivity of the streams in both compartments during one full cycle. During the first half cycle, the conductivity in compartment A increased while conductivity in compartment B decreased. In the second half cycle, the opposite trend was observed. This clearly shows the ability of the device to concentrate LiCl in one compartment and dilute it in the same magnitude in the other compartment. Fig. 5b shows that this behavior was stable over longer periods of time.

A quantitative assessment of the ion removal capacity of our cell was conducted using Ion Chromatography (IC). With this aim, samples were taken in each tank before and after one half-cycle, and subsequently analyzed by IC.

A lithium adsorption capacity (SAC_{Li}) of 27 $mg_{Li}\ g_{LFP}^{-1}$ and an areal adsorption capacity (AAC) of 9 $g_{Li}{\cdot}m^{-2}$ were obtained along with a η of 80% when operating the system at 3 mA cm^{-2}. Note that these figures of merits are defined in the Experimental Section. Whereas these values are comparable to the values reported in literature [10], the use of semi-solid electrode allows not only an easy regeneration of the systems but also the achievement of unprecedented values of areal capacities (3–4 mAh cm^{-2}), which is a key parameter for practical implementation of this electrochemical technology reducing installation cost per kg of Li (Fig. S8) and minimizing ion mixing between half-cycles. Furthermore, Li permeability tests conducted for the anion selective membrane used in this work (Section S8) revealed that Li ions were able to cross over it, which contributed negatively to the efficiency. Thus, anion selective membrane are not only expensive elements (Section S5), but their ability to confine small cations such as Li-ion is not sufficiently high. This motivated us to extend the concept of REIPC to a membrane-free configuration: The Membrane-Free Regenerative Ion Pumping Cell (MF-REIPC).

3.3. *Membrane-Free Regenerative Electrochemical Ion Pumping Cell (MF-REIPC)*

Selectivity towards specific ions is also achieved by using two ion-selective Faradaic materials without the need for ion-selective

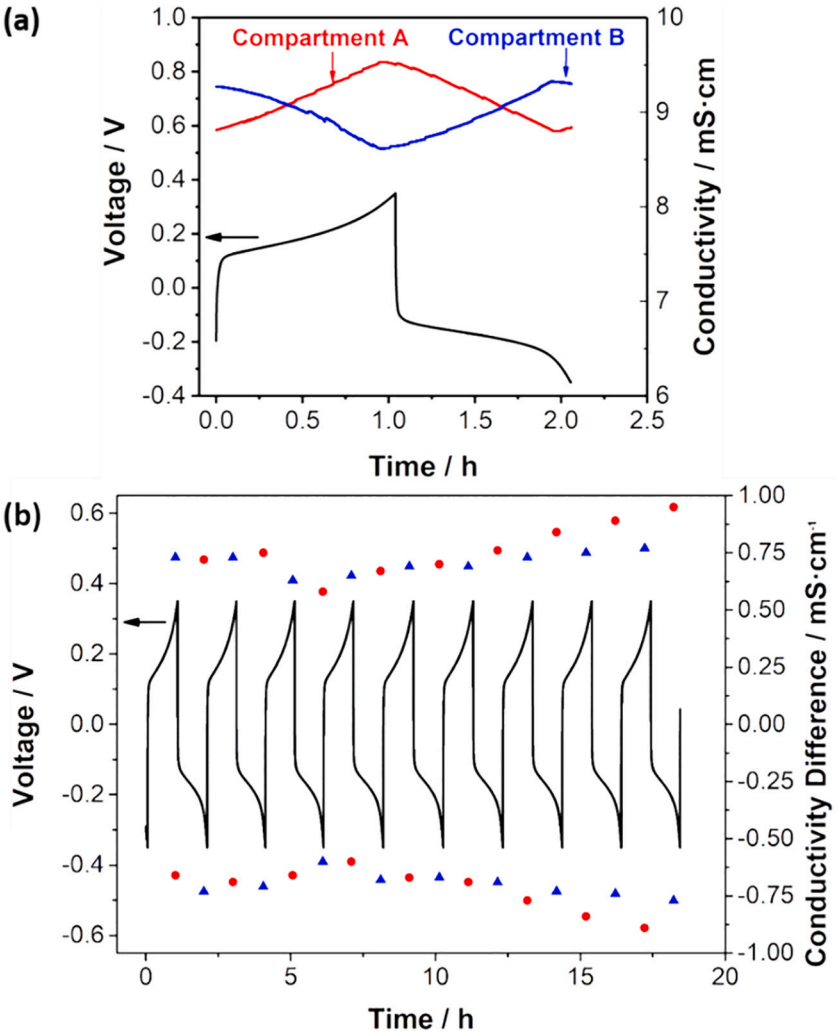

Fig. 5. Evolution of cell voltage and ionic conductivity of the symmetrical REIPC during (a) one full cycle and (b) ca. 20 h. Blue triangles and red circles represent the conductivity difference values in each one of the compartments at the end of each one of the charging/discharging cycles. (For interpretation of the references to colour in this figure legend, the reader is referred to the web version of this article.)

membranes, as discussed above [23,30]. As a result, this section is dedicated to developing a Membrane-Free Regenerative Electrochemical Ion Pumping Cell (MF-REIPC). This concept consists of an asymmetrical cell configuration that introduces a significant cost reduction by removing the ion-selective membrane while having the ability of separating specific ions and storing energy (Fig. 1b). In Supp. Info. Section S2 Fig. S3 describes the different elements in the cell design for this concept. The Faradaic materials selected for this system were Nickel Hexacyanoferrate (NiHCF, $KNiFe(CN)_6$) and Lithium Manganese Oxide (LMO, $LiMn_2O_4$). By using a Na-selective material, i.e. NiHCF, [31] and a Li-selective material, i.e. LMO, the ion-selective membrane is no longer needed to provide ion selectivity to the system [5].

In this concept, the process started by injecting a LMO semi-solid electrode in the pre-assembled cell followed by oxidation of LMO ($LiMn_2O_4$) to MO (Mn_2O_4). Details of this oxidation process ("activation") are provided in Supp. Info. (Section S3). Once the oxidation process was completed, a NiHCF semi-solid electrode was injected in the opposite compartment. Ion removal in the MF-REIPC consists of two steps: in the charge step, Li-ions are released by the LMO electrode in the stream leading to an increase in Li-ion concentration in the stream. Simultaneously, the NiHCF electrode captures Na-ions resulting in a decrease in Na-ion concentration in the stream. (Section S10, Fig. S13 (a-c) Supp. Info.). In the discharge step, the opposite process takes place i.e., Na-ions are released, and Li-ions are captured (Section S10, Fig. S13 (d-e) Supp. Info.) leading to a Na-ion concentrated and Li-ion diluted stream.

Since the distinct feature of the proposed technology is the possibility of regenerating the systems by substituting the spent semi-solid electrodes once the battery reaches its end-of-life, regeneration capability of the system was first evaluated. A MF-REIPC using LMO-NiHCF active materials was studied for ion separation in a stream containing 0.1 M NaCl and 0.1 M LiCl in one single solution tank (Fig. S3 Supp. Info.). It should be noted that a batch configuration with only one tank, instead of using two tanks, was set up. The initially assembled MF-REIPC system having NiHCF and LMO semi-solid electrodes was run for 28 cycles. Then, the following regenerations were carried out (Fig. 6a): R1) LMO was replaced by a semi-solid electrode that only contained carbon additive (without Faradaic material). Consequently, the Faradaic behavior initially observed (cycle 1–28) turned into a capacitive behavior (cycle 29–52) leading to a sloppier voltage profile (Fig. 6b). As the specific charge capacity of carbon additive is lower than that of LMO, the charge capacity of the system decreased by 75% when carbon semi-solid electrode replaced LMO semi-solid electrode. R2) The carbon-based semi-solid electrode was replaced by a fresh LMO semi-solid electrode while the NiHCF semi-solid electrode was substituted by a fresh one having the same formulation. Fig. 6a shows that the system was able to recover the initial charge capacity value (3.5 mAh cm^{-2}). These results confirm the versatility and robustness of the proposed concept as demonstrated by

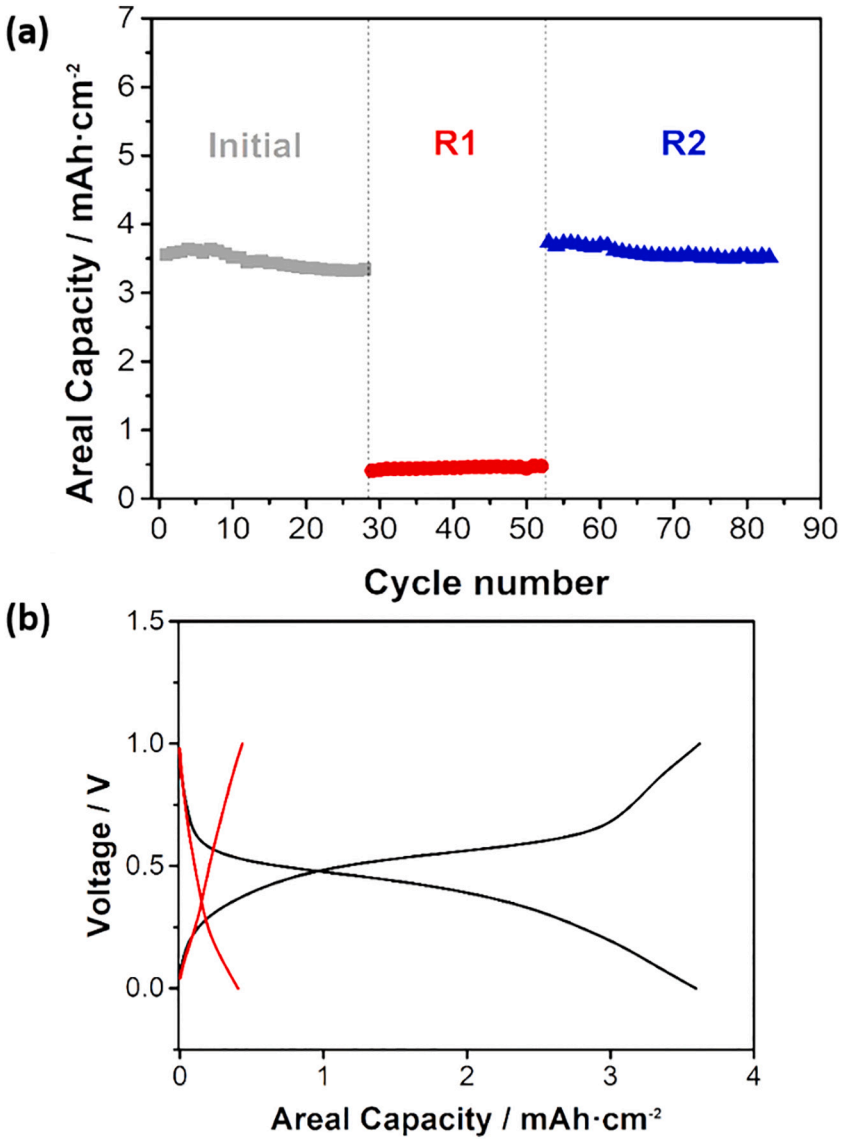

Fig. 6. (a) Evolution of the areal capacity of the MFREIPC LMO-NiHCF cell with the number of cycles. Regenerations were conducted in cycle 28 (carbon-based semi-solid electrode replaced NiHCF semi-solid electrode) and cycle 52 (fresh semi-solid electrodes). (b) Comparison between capacitive (Activated Carbon-Activated Carbon, red line) and Faradaic (LMO-NiHCF, black line) MF-REIPC. Note that areal capacity (mAh cm^{-2}) is estimated as the accumulated charge (mAh) provided by the potentiostat during one step normalized by the geometric area of the electrodes. (For interpretation of the references to colour in this figure legend, the reader is referred to the web version of this article.)

the possibility of replacing electrode active materials for the same assembled cell. Fig. S14 (Section S11) shows the long-term stability of the system delivering a capacity fading of 0.13% $cycle^{-1}$ and 0.022% h^{-1} over 160 cycles and 1.000 h. It should be noted that we did not observe any coloring or suspended particles after 6 weeks operating in batch (using the same solution), which confirmed that Celgard separator effectively confines solid materials. Future studies will explore whether the use of Celgard is more effective to confine solid materials in the electrodes compared to the conventional use of binder.

The ion separation capacities of the system were first evaluated using

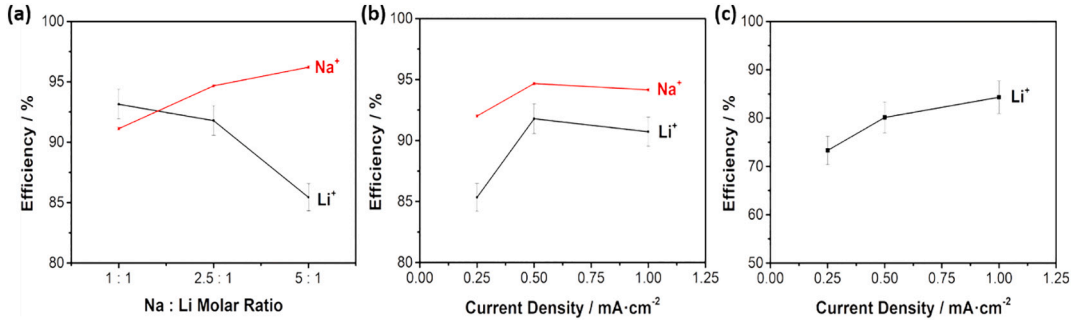

Fig. 7. Efficiencies obtained with MF-REIPC (a) Effect of the Na:Li ions ratio in the solution for a current density of 0.5 mA cm^{-2}. (b) Effect of the current density for a Na:Li ratio of 2.5:1.0 (c) Impact of the presence of additional cations on Lithium capturing using Atacama brine solution. Charge steps were carried out at constant current density to avoid potential interfering of oxygen evolution reaction, so that the influence of the current density on the efficiency process was evaluated for the discharge step.

a solution containing only Na-ions and Li-ions, and then a solution emulating the brine of Atacama Lake (43 mM Li^+, 757 mM Na^+, 102 mM K^+ and 66 mM Mg^{2+} [11]). Fig. 7a shows the evolution of the efficiency with the ratio between concentration of Na-ions and Li-ions. As expected, increasing ratio of Na:Li led to an increase in the efficiency for Na-ions and a decreased for Li-ions. Thus, the efficiency for brine samples in which the concentration of Li-ions is lower than that of Na-ions will be determined by the selectivity of the Li-capturing material (LMO in our case). The Li selectivity (normalized values varying between 0 and 1) followed similar trend as the Li efficiency, since it decreased with increasing concentration of Na-ions at 0.5 mA cm^{-2} (Fig. S13). Since the Li selectivity is determined by the intrinsic selectivity of the intercalations materials, the results indicate that there is room for improvement by optimizing electrode parameters and operating conditions. The influence of the current density, which is critical for the cost, was also evaluated (Fig. 7b). The efficiency for both Li-ions and Na-ions increased with increasing current density (from 0.25 to 0.5 mA cm^{-2}), which is attributed to the kinetics of ion-intercalation processes. As current density increases, the kinetically hindered processes are unfavored making LMO and NiHCF more selective towards Li-ions and Na-ions, respectively. Unfortunately, another 2-fold increase in current density from 0.5 to 1 mA cm^{-2} did not result in further improvement in efficiency. When working with solutions containing 0.1 M LiCl and 0.25 M NaCl at 0.5 mA cm^{-2}, the efficiencies were above 90% (94% and 92% for Na-ions and Li-ions, respectively), achieving an areal capacity of 2.6 mAh cm^{-2}, SAC_{Li} of 16.2 mgLi·g_{NiHCF}^{-1}, AAC of 4 g_{Li} m^{-2} and energy consumption of 15.6 Wh·mol^{-1}. Comparison of the performances achieved in this work with other values reported in the literature (Table S1) suggests that the proposed REIP systems is competitive with other non-regenerative systems.

Finally, a solution emulating the brine of Atacama was studied (Fig. 7c). Only Li-ions were analyzed in this case due to the difficulties of measuring reliably both Li-ions and Na-ions with such a large difference in concentration by flame photometry. The efficiency increased continuously in the range of 0.25–1.00 mA cm^{-2}, while the ion separation capacity showed a maximum at 0.50 mA cm^{-2}. At this current density, an efficiency of 81%, an ion separation capacity of 0.17 g_{Li}· h^{-1} m^{-2}, specific capacity of 61.6 mAh·g_{NiHCF}^{-1} and consumption of 27 Wh L^{-1} was obtained Note that our estimations include both steps (charge and discharge). Again, whereas these values are comparable to the values reported in literature [32], the use of semi-solid electrode allows not only easy regeneration of the systems but also achievement of unprecedented values of areal capacities (3–4 mAh cm^{-2}), which is a key parameter for practical implementation of this electrochemical technology reducing installation cost per kg of Li (Fig. S8). For continuous Li recovery, an electro-valve controlled by a programmable logic controller (PLC) could swap the streams to achieve continuous Li extraction. A small mixing of Li-rich and Li-poor solutions occurs upon the swapping decreasing the overall efficiency would be expected, as experienced before by Palagonia et al. [26]. Moreover, we could anticipate that our high areal capacity electrodes, able to retain a larger amount of Li per area, will help minimizing these losses. It should be noted that, in our experiment, solution exchange was not carried out between half-cycles. As a consequence, the energy consumption (27 Wh mol_{Li}^{-1}) was higher than some of the previous values reported in the literature. Small volumes were used to reliably measure the concentration changes, so that the concentration during Li uptake step continuously decreases. This detrimental decrease in Li concentration during Li uptake step does not occur when large volumes of brine are employed as in report in the literature. This highlights the difficulties when benchmarking performance, especially in terms of energy consumption. In any case, our prototype delivered competitive electrochemical and ion separation performances, whereas providing the ability of easy regeneration when reaching end-of-life.

In summary, a new ion capturing and separation device, REIPC, which consists of an electrochemical cell equipped with injectable battery type electrodes able to selectively capture and concentrate the ions of interest, was successfully demonstrated. The injectable electrodes enable improving the recyclability and direct reuse of the cell without affecting negatively to the electrochemical performance. In this sense, the techno-economic analysis indicated that a 95% of the fabrication cost is reduced in each regeneration of the semisolid electrodes by recycling the passive components of the cell. Additionally, the operation of the REIPC is based on electrochemical phenomena, which does not require the use of extraction agents to elute the ion captured from the active material. These aspects represent a tremendous impact of this technology from the sustainability point of view with respect to the precipitation and ion exchange resins processes.

Furthermore, the REIPC system developed in this research is exceptionally versatile since it can be equipped with different kind of electrodes allowing to capture different type of ions. Thus, our results show that modifications in cell voltage and ion selectivity can be achieved by simply replacing the active materials. Indeed, we show that the combination of different electrode materials and/or membranes opens the possibility to store energy while capturing ions (asymmetrical configuration). Furthermore, a membrane-free configuration using two electrodes selective to different ions (as it is the case of the MF-REIPC system equipped with LMO and NiHFC electrodes) accomplished a remarkable performance, not only when tested in dual electrolytes, but also when running experiments using solutions that emulate typical Atacama's brine compositions. Hence, this versatility opens the path for exploring the application of this technology to other solutions to be treated in different fields such as battery recycling, water treatment plants, waste valorization, agricultural business or pharmaceutical applications.

CRediT authorship contribution statement

Daniel Perez-Antolin: Methodology, Experimental work, Investigation, Visualization, Writing- Original draft. **Cristina Irastorza**: Investigation, Experimental Work **Sara Gonzalez:** Investigation, Experimental Work. **Rebeca Moreno:** Investigation, Experimental Work **Garcia-Quismondo:** Supervision, Writing - Review **Jesús Palma**: Supervision, Writing - Review Funding acquisition. **Julio J. Lado:** Conceptualization, Methodology, Writing - Review & Editing, Supervision, Funding acquisition. **Edgar Ventosa**: Conceptualization, Methodology, Writing - Review & Editing, Supervision, Funding acquisition.

Funding sources

J.J. Lado acknowledges Comunidad de Madrid for the postdoctoral fellowship as part of the Young Talent Attraction Program (2020-T1/AMB-19799).

E. Ventosa acknowledges the financial support by the Spanish Government through the Research Challenges Programme (Grant RTI2018-099228-A-I00), Ramon y Cajal Programme (RYC2018-026086-I) as well as “la Caixa” Foundation (LCF/PR/PR18/51130007).

Declaration of competing interest

The authors declare that they have no known competing financial interests or personal relationships that could have appeared to influence the work reported in this paper.

Acknowledgment

The authors would like to acknowledge the technical work performed by Ignacio Almonacid and Guzman García on the software development and construction of the REIPC cell system. The authors also would like to thank Gonzalo Castro for collaborating in the laboratory experiments and the sample analysis.

Appendix A. Supplementary data

Supplementary data to this article can be found online at https://doi.org/10.1016/j.desal.2022.115764.

References

[1] Lithium 2019 Recharge - Canaccord Genuity, (n.d.). http://cdn.ceo.ca.s3-us-west-2.amazonaws.com/1eo071m-Canaccord - Neo Lithium Corp Researn Note - Sept 2019.pdf.

[2] I. Energy Agency , Global EV Outlook 2020 Entering the Decade of Electric Drive?, (n.d.).

[3] E.J. Calvo, Electrochemical methods for sustainable recovery of lithium from natural brines and battery recycling, Curr. Opin. Electrochem. 15 (2019) 102–108, https://doi.org/10.1016/j.coelec.2019.04.010.

[4] P. Meshram, B.D. Pandey, T.R. Mankhand, Extraction of lithium from primary and secondary sources by pre-treatment, leaching and separation: a comprehensive review, Hydrometallurgy 150 (2014) 192–208, https://doi.org/10.1016/j.hydromet.2014.10.012.

[5] R. Trócoli, C. Erinmwingbovo, F. La Mantia, Optimized lithium recovery from brines by using an electrochemical ion-pumping process based on λ-MnO2 and nickel hexacyanoferrate, ChemElectroChem 4 (2017) 143–149, https://doi.org/10.1002/celc.201600509.

[6] L. Kong, X. Liu, Emerging electrochemical processes for materials recovery from wastewater: mechanisms and prospects, Front. Environ. Sci. Eng. 14 (2020) 1–14, https://doi.org/10.1007/s11783-020-1269-2.

[7] Lithium Extraction Technologies, Tech 2018S11. Nexant (n.d.), https://www.nexanteca.com/file/137456/download?token=NeqrmzjJ, November 2018.

[8] M. Pasta, A. Battistel, F. La Mantia, Batteries for lithium recovery from brines, Energy Environ. Sci. 5 (2012) 9487–9491, https://doi.org/10.1039/c2ee22977c.

[9] M.E. Suss, V. Presser, Water desalination with energy storage electrode materials, Joule 17 (2018) 10–15, https://doi.org/10.1016/j.joule.2017.12.010.

[10] A. Battistel, M.S. Palagonia, D. Brogioli, F. La Mantia, R. Trócoli, Electrochemical methods for lithium recovery: a comprehensive and critical review, Adv. Mater. 32 (2020), 1905440, https://doi.org/10.1002/adma.201905440.

[11] R. Trõcoli, A. Battistel, F. La Mantia, Nickel hexacyanoferrate as suitable alternative to ag for electrochemical lithium recovery, ChemSusChem 8 (2015) 2514–2519, https://doi.org/10.1002/cssc.201500368.

[12] J.S. Kim, Y.H. Lee, S. Choi, J. Shin, H.C. Dinh, J.W. Choi, An electrochemical cell for selective lithium capture from seawater, Environ. Sci. Technol. 49 (2015) 9415–9422, https://doi.org/10.1021/acs.est.5b00032.

[13] H. Yoon, J. Lee, S. Kim, J. Yoon, Review of concepts and applications of electrochemical ion separation (EIONS) process, Sep. Purif. Technol. 215 (2019) 190–207, https://doi.org/10.1016/j.seppur.2018.12.071.

[14] Z.H. Huang, Z. Yang, F. Kang, M. Inagaki, Carbon electrodes for capacitive deionization, J. Mater. Chem. A 5 (2017) 470–496, https://doi.org/10.1039/c6ta06733f.

[15] Y. Liu, C. Nie, X. Liu, X. Xu, Z. Sun, L. Pan, Review on carbon-based composite materials for capacitive deionization, RSC Adv. 5 (2015) 15205–15225, https://doi.org/10.1039/c4ra14447c.

[16] J.J. Wouters, M.I. Tejedor-Tejedor, J.J. Lado, R. Perez-Roa, M.A. Anderson, Influence of metal oxide coatings on the microstructural and electrochemical properties of different carbon materials, J. Electrochem. Soc. 163 (2016), https://doi.org/10.1149/2.0911613jes. A2733-A2744.

[17] J.J. Wouters, M. Isabel Tejedor-Tejedor, J.J. Lado, R. Perez-Roa, M.A. Anderson, Influence of metal oxide coatings, carbon materials and potentials on ion removal in capacitive deionization, J. Electrochem. Soc. 165 (2018), https://doi.org/10.1149/2.0271805jes. E148-E161.

[18] C. Santos, J.J. Lado, E. García-Quismondo, I.V. Rodríguez, D. Hospital-Benito, J. Palma, M.A. Anderson, J.J. Vilatela, Interconnected metal oxide CNT fibre hybrid networks for current collector-free asymmetric capacitive deionization, J. Mater. Chem. A 6 (2018) 10898–10908, https://doi.org/10.1039/c8ta01128a.

[19] J.J. Lado, R.L. Zornitta, I.Vázquez Rodríguez, K.Malverdi Barcelos, L.A.M. Ruotolo, Sugarcane biowaste-derived biochars as capacitive deionization electrodes for brackish water desalination and water-softening applications, ACS Sustain. Chem. Eng. 7 (2019) 18992–19004, https://doi.org/10.1021/acssuschemeng.9b04504.

[20] K. Singh, S. Porada, H.D. de Gier, P.M. Biesheuvel, L.C.P.M. de Smet, Timeline on the application of intercalation materials in capacitive deionization, Desalination 455 (2019) 115–134, https://doi.org/10.1016/j.desal.2018.12.015.

[21] J. Lee, S. Kim, J. Yoon, Rocking chair desalination battery based on prussian blue electrodes, ACS Omega 2 (2017) 1653–1659, https://doi.org/10.1021/acsomega.6b00526.

[22] F. Yu, L. Wang, Y. Wang, X. Shen, Y. Cheng, J. Ma, Faradaic reactions in capacitive deionization for desalination and ion separation, J. Mater. Chem. A 7 (2019) 15999–16027, https://doi.org/10.1039/C9TA01264H.

[23] K. Singh, Z. Qian, P.M. Biesheuvel, H. Zuilhof, S. Porada, L.C.P.M. de Smet, Nickel hexacyanoferrate electrodes for high mono/divalent ion-selectivity in capacitive deionization, Desalination 481 (2020), 114346, https://doi.org/10.1016/j.desal.2020.114346.

[24] M. Duduta, B. Ho, V.C. Wood, P. Limthongkul, V.E. Brunini, W.C. Carter, Y. M. Chiang, Semi-solid lithium rechargeable flow battery, Adv. Energy Mater. 1 (2011) 511–516, https://doi.org/10.1002/aenm.201100152.

[25] E. Ventosa, D. Buchholz, S. Klink, C. Flox, L.G. Chagas, C. Vaalma, W. Schuhmann, S. Passerini, J.R. Morante, Non-aqueous semi-solid flow battery based on na-ion chemistry. P2-type NaxNi0.22Co0.11Mn0.66O2-NaTi2(PO4)3, Chem. Commun. 51 (2015) 7298–7301, https://doi.org/10.1039/c4cc09597a.

[26] M.S. Palagonia, D. Brogioli, F. La Mantia, Lithium recovery from diluted brine by means of electrochemical ion exchange in a flow-through-electrodes cell, Desalination 475 (2020), https://doi.org/10.1016/j.desal.2019.114192.

[27] Z. Guolang, C. Linlin, Y. Chao, X. Li, G. Zhou, L. Chen, G. Luo, W. Zhu, Progress in electrochemical lithium ion pumping for lithium recovery, Artic, J. Energy Chem. 59 (2020) 431–445, https://doi.org/10.1016/j.jechem.2020.11.012.

[28] K.B. Hatzell, M. Boota, Y. Gogotsi, Materials for suspension (semi-solid) electrodes for energy and water technologies, Chem. Soc. Rev. 44 (2015) 8664–8687, https://doi.org/10.1039/c5cs00279f.

[29] R. Trócoli, A. Battistel, F. La Mantia, Selectivity of a lithium-recovery process based on LiFePO4, Chem. Eur. J. 20 (2014) 9888–9891, https://doi.org/10.1002/chem.201403535.

[30] W. Shi, P. Nie, X. Shang, J. Yang, Z. Xie, R. Xu, J. Liu, Berlin green-based battery deionization-highly selective potassium recovery in seawater, Electrochim. Acta 310 (2019) 104–112, https://doi.org/10.1016/j.electacta.2019.04.122.

[31] S. Porada, A. Shrivastava, P. Bukowska, P.M. Biesheuvel, K.C. Smith, Nickel hexacyanoferrate electrodes for continuous cation intercalation desalination of brackish water, Electrochim. Acta 255 (2017) 369–378, https://doi.org/10.1016/j.electacta.2017.09.137.

[32] X. Zhao, H. Yang, Y. Wang, Z. Sha, Review on the electrochemical extraction of lithium from seawater/brine, J. Electroanal. Chem. 850 (2019), 113389, https://doi.org/10.1016/j.jelechem.2019.113389.